

# Development Process of a Numerical Simulation for the Hammer Peening Fatigue Life Improvement Technique

BAPTISTA, R.\*, INFANTE, V.\*\*, BRANCO, C.M.\*\*

\*Department of Mechanical Engineering, Escola Superior de Tecnologia de Setúbal (IPS)  
Campus do IPS, Estefanilha, 2910-761 Setúbal, Portugal

\*Corresponding author email: [r.baptista@est.ips.pt](mailto:r.baptista@est.ips.pt)

\*\*ICEMS/IST, Lisbon University of Technology, Av. Rovisco Pais, 1049-001  
Lisbon, Portugal

## Abstract

Most rehabilitation and fatigue life improvement techniques of welded structures were developed in the 60's and 70's, when the problems introduced by the welding processes were brought up to light, by the first major accidents involving this type of structures. Nowadays, when the budgets for the experimental analysis are tighter, it is fundamental to use new simulation tools, with the principal objective of developing the fatigue life improvement techniques of welded structures.

The work presented in this paper, intends to demonstrate the viability of the finite element analysis simulation of one of the most important fatigue life improvement techniques of welded structures, the *Hammer Peening*.

It was already experimentally demonstrated that this technique allows for the treated structure to have a fatigue life equal or superior to the original one, due to the introduction of a local compressive residual stress field. Considering the difficulties encountered in the experimental determination of residual stresses introduced by this technique, the computational simulation stands out as a strong alternative to experimental analysis and development.

The residual stress fields were obtained numerically on the welded structure, using elasto-plastic material models and considering an elastic-deformable hammering tool. Several parameters of this technique were considered variable, and its influence was analysed in the simulation process, allowing for a good agreement with the experimental results.

The major advantage of the computational simulation of the hammering technique is the possibility of adding to the obtained results, a nominal load on the welded joint. Thereby it is possible to predict the fatigue life improvement, introduced by hammering, as a function of the parameters used in the process.

Key-words: Hammer Peening; Fatigue Life; Improvement; Finite Element Analysis

## 1 Introduction: Background

In order to reduce the cost of developing a new fatigue life improvement technique, and therefore reduce the cost of operating a more secure welded structure, the correct modeling using a FEA program is essential. These programs can nowadays easily simulate almost every detail and effect present on the experimental test runs, and a fatigue life improvement technique [1] and [2], like the hammer peening can be modeled.

Several developments have already been made by *Baptista and Infante*, on [3] and [4], in order to produce accurate simulation of this technique, and its experimental application on [5] and [6]. But most recently on [7] an extensive study on the application of several fatigue life improvement techniques on stainless steels welded joints, have been presented.

Fatigue life improvement techniques rely on extending the initiation phase, by reducing the severity of the weld toe details or introducing a compressive residual stress field [8]. Improvement techniques also reduce the crack propagation speed; which increases the total fatigue life of the structure. In a review recently presented by Maddox [9], conclusions and recommendations were defined for hammer peening which is now part of an official IIW document of Commission XIII [10].

In the present work the full development process of a simulation analysis of the hammer peening technique is described, like in [11], taking into account the latest developments on the fatigue life prediction methods [12]. This technique will be modeled using a deformable hammering tool and several experimental results, in order to make it closer to the real process. Finally the numerical results are compared with the ones obtained experimentally, in order to validate the numerical model.

## 2 Experimental and Numerical Data

### 2.1 Material and Specimens

The first step for an accurate modeling of the hammer peening fatigue life improvement technique, using FEA, is to obtain a numerical model for the material behavior. There is one material in study within this work, a Stainless Steel, referred as Duplex Type S31803 (DIN 1.4462). In Table 1 the chemical composition of this material can be found. Table 2 gives us the normal tensile properties of this duplex steel, becoming clear that this material has a high ultimate stress, 789 MPa, and shows a 34% elongation at break point.

The material was received in as welded condition, with a plate thickness of 10 mm and the simplified specimen geometry can be found in Figure 1

**Table 1 Chemical Composition of Duplex S31803 Stainless Steel**

C	Si	Mn	P	S	Cr
0.024	0.220	1.550	0.023	0.002	22.400
Mo	Ni	N	Al	Cb	Cu
2.980	5.700	0.157	-	0.130	0.090

**Table 2 Tensile Properties**

Steel	$\sigma_{0.2\%}$ [MPa]	$\sigma_R$ [MPa]	$\epsilon_R$ [%]
S31803	478	789	34

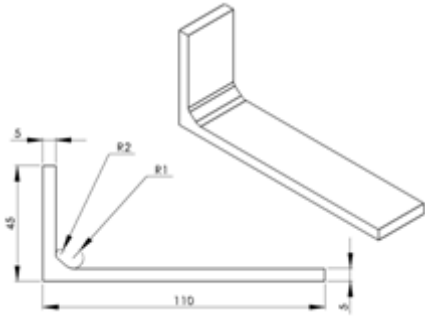


**Figure 1 Simplification of the cruciform welded joint specimen**

## 2.2 Numerical Material Models

These properties must be translated in to a numerical model using a FEA program, therefore a complete elasto-plastic material model is necessary. From all the models included on the ABAQUS material library, the “Linear kinematic hardening model” and the “Nonlinear isotropic/kinematic hardening model”, are the ones that offer the most complete behavior for a FEA of cyclic fatigue test. When a Nonlinear and Kinematic hardening model are combine, the *Lemaitre and Chaboche* [13] is obtained and therefore the most complete cyclic behavior can be simulated. Effects like the Bauschinger effect, Cyclic hardening with plastic shakedown, Ratchetting and the Relaxation of the mean stress, can be easily simulated by this model, considering one has the full sets of parameters that define the Chaboche model. Table 3 shows the parameters for a Chaboche model, were the parameters were calibrated from experimental results.

**Table 3 Duplex Steel Chaboche material model [14]**

$E$ [MPa]	$\nu$	$\sigma_{0.2\%}$ [MPa]	$C$	$Q_{\infty}$	$b$
179000	0.3	187.6	134771	16.5	0.0073

Finally in order to apply the local approach method, [15], a Cyclic stress-strain curve is also necessary, equations ( 1 ) and ( 2 ) express the Ramberg-Osgood, model for the Duplex Steel, and a Morrow’s modified strain-life equation, [16], ( 3 ) and ( 4 ), is also required for fatigue life initiation prediction. All these equations are based on experimental data obtained in order to calibrate the material models by *Magnabosco* [17].

$$\frac{\Delta \epsilon}{2} = \frac{\Delta \sigma}{2E} - \left( \frac{\Delta \sigma}{2H} \right)^{1/n} \quad (1)$$

$$\frac{\Delta \epsilon}{2} = \frac{\Delta \sigma}{2 \cdot 179000} - \left( \frac{\Delta \sigma}{2 \cdot 733} \right)^{1/0.383} \quad (2)$$

$$\frac{\Delta \epsilon}{2} = \left( \frac{\sigma_f - \sigma_m}{(2N)^b} - \epsilon' (2N)^{c'} \right) \quad (3)$$

$$\frac{\Delta \epsilon}{2} = \frac{(912 - \sigma_m)}{179000} (2N)^{0.383} - 0.254 (2N)^{-0.477} \quad (4)$$

## 2.3 Geometry and Boundary Conditions

The referred specimen geometry was then model using the ABAQUS design tools, using a 1/8 symmetry simplification in order to reduce the problem computational load, and the data on table Table 4. The values for the weld toe radii (R1), the weld toe angle, and the secondary radii (R2) were obtained from a experimental geometry analysis, using a digital coordinate table and were then statistically analyzed. A average value of 2.420 mm was obtained for the weld toe radii, after the weld toe hammer peening vs. the as welded value of 1.645 mm. The standard deviation (0.683 mm) value was then used to generate four other numerical specimens, by increasing and decreasing the value of R1, in order to quantify its effect on the fatigue life prediction.

**Table 4 Stress Concentration Factors, obtained for a 250 MPa nominal Stress**

Specimen	R1 [mm]	Angle [°]	R2 [mm]	$K_t$
ProvAvg02Std	1.053			1.952
ProvAvg01Std	1.737			1.770
ProvAvg	2.420	38.238	1.645	1.678
ProvAvg1Std	3.104			1.565
ProvAvg2Std	3.787			1.502

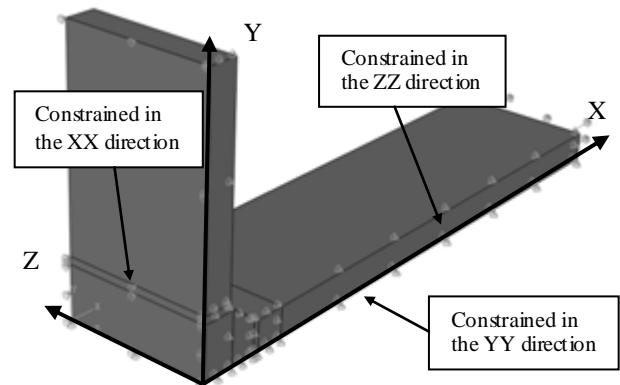


**Figure 2 FEA Model and coordinate system and Boundary conditions**

The model was constrained using the boundary conditions on Figure 2, that fix the model in space accordingly to the specimen symmetry conditions. Taking into account the non linear nature of the hammer peening technique, which includes a non linear material model, a contact condition and finally a dynamically applied load, like *J. Liu* in [18] recommended, the specimen wide had to be reduced from 25 mm to 1.125 mm, in order to get the best ratio between the quality of the results and the computational effort. Therefore both lateral surfaces were restrained in the ZZ (or transverse)

direction, to simulate the specimen plane strain state. Using a nominal 250 MPa stress it was also possible to calculate the stress concentration factor for the longitudinal direction (Table 4) as a way to quantify the influence of the weld toe radii.

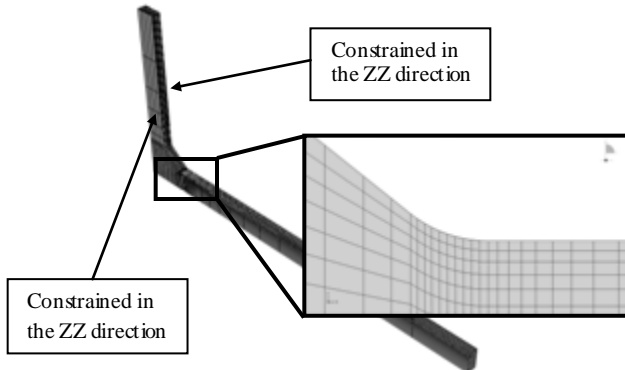


**Figure 3 1.125 mm wide model**

## 2.4 Specimen Mesh

In order to evaluate the influence of the specimens mesh on the quality of the final results, three meshes were developed, the first one had only 2'016 C3D8R elements, which are linear elements and therefore this coarse mesh had 8'127 DOF. A medium and fine mesh were then developed, using 15'855 and 26'103 DOF. The results showed that the coarse mesh does not allow obtaining consistent results, but the medium and fine meshes both resulted on very similar stress and strain distributions. Once again in order to reduce the computational effort, the medium mesh was then used from this point forward.

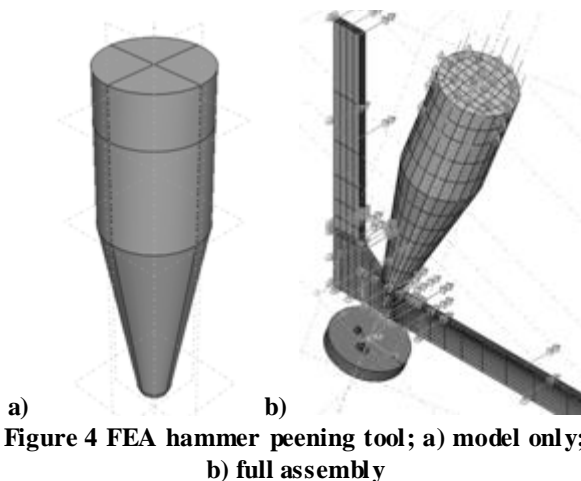


**Figure 4 FEA hammer peening tool; a) model only; b) full assembly**

Finally a 12 mm in diameter hammer peening tool was defined using a linear elastic material model, but the full body is deformable. Figure 4 shows the tool geometry, next to the weld toe, and the applied boundary conditions. The tool mesh uses the same element and adds 3'798 DOF to the simulation. A contact pair was also defined between the tool (master surface) and the specimen (slave surface), using a hard contact model, that allows separation after contact, for the normal to

surface direction, and a penalty model, with a 0.5 friction coefficient, for the tangential direction.

## 2.5 Hammer Peening Loads

The next required step was to determine the hammer peening force, needed to be applied to the numerical tool. This was done experimentally using a hammer peening tool instrumented with two strain gages; these were calibrated using a servo-hydraulic test machine, in order to translate one hammer peening run, in a load spectrum, Figure 5.

This spectrum was analyzed using the Rain-flow method and four characteristic loading cycles were defined. Table 5 shows not only these 4 loading sets, with loads ranging from 1.9 to 9.5 MPa, but also the corresponding residual stresses on the weld toe, when 4 hammering runs, each one with 5 strokes, are applied to the 1.125 mm wide specimen. The strokes were applied using the referred loads, dynamically applied on the top of the hammer peening tool, with a 0.02 Hz frequency.

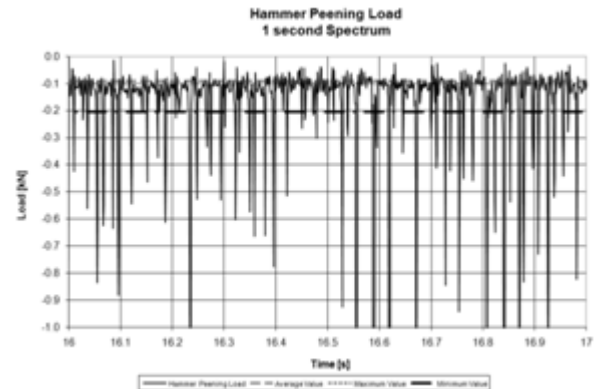


**Figure 5 Hammer Peening Load 1 second spectrum**

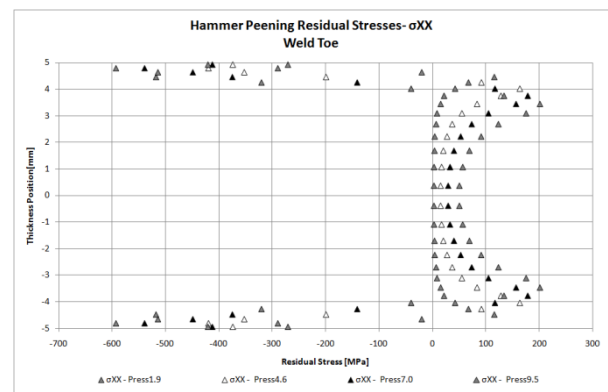


**Figure 6 Residual Stress distribution, after the hammer peening process**

Figure 6 shows the stress distribution in the longitudinal direction on the weld toe vs. the hammering load. A minimum value of - 592.8 MPa is obtained with a 9.5 MPa load, and a maximum residual stress of - 290.0 MPa for the 1.9 MPa load.

An experimental value of – 485 MPa was obtained for the residual stresses on the duplex steel using X-Ray Diffraction technique in the longitudinal direction, and – 524 MPa in the transverse direction. One can then conclude that the best solution for a numerical simulation of the hammer peening technique is the 7.0 MPa loading set. Finally it is possible to check that the compressive stress influence is about 0.5 mm to 1 mm throughout the specimen thickness.

**Table 5 Weld toe Residual Stress vs. Hammer peening load**

Specimen	$\sigma_{XX}$ [MPa]	$\sigma_{YY}$ [MPa]	$\sigma_{ZZ}$ [MPa]
Press1.9	-290.0	-103.5	-243.4
Press4.6	-418.9	-101.3	-430.2
Press7.0	-538.9	-116.8	-506.9
Press9.5	-592.8	-162.0	-580.6

On the other hand, one can see in Table 6 that after a nominal load with a stress range of 225 MPa and a stress ratio of 0.1, the local stress and strain ranges are not significantly influenced by the hammering load. Only the mean stress is considerably lower (about 71 %) when a 1.9 MPa load is applied, but only 5.5 % higher when a 9.0 MPa load is applied vs. the 7.0 MPa load, used from this point on.

**Table 6 Weld toe local stress range, mean stress and strain range vs. Hammer peening load**

Specimen	$\Delta\sigma_{XX}$ [MPa]	$\sigma_{mXX}$ [MPa]	$\Delta\epsilon_{XX}$ [ $\mu$ ]
Press1.9	348.9	-54.5	1933
Press4.6	368.4	-142.8	2007
Press7.0	365.1	-185.7	1969
Press9.5	366.9	-195.9	1958

### 3 Results and Discussion

#### 3.1 Residual Stress in the Welded Joints

Using the above referred specimen wide, hammer peening tool tip radii, positioning and load, the 4 runs of 5 hammering strokes were applied to the five specimens with different weld toe radii from Table 4.

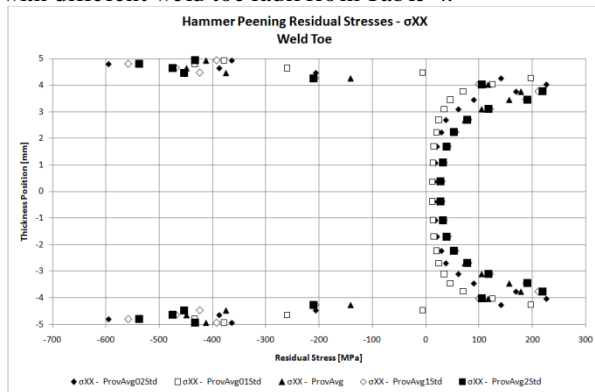


**Figure 7 Residual Stress distribution, after the hammer peening process, vs. weld toe radii**

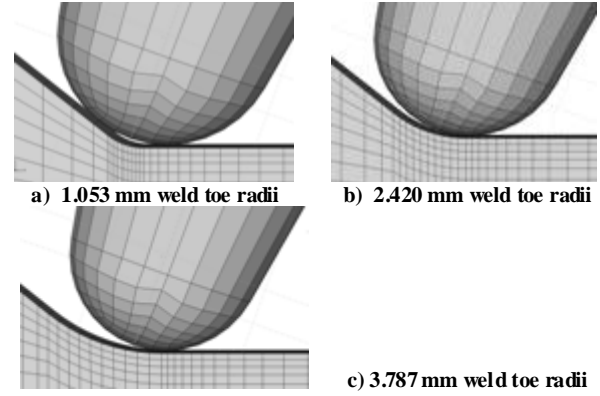


**Figure 8 Weld toe radii vs. Hammer peening tool radii**

Figure 7 shows the influence of the weld toe radii on the residual stress distribution on the longitudinal direction, at the weld toe. On the two smaller weld toe radii specimens the stress distribution is clearly different from the other three ones. The smaller radii means the tool tip cannot hammerpeen directly above the weld toe, as one can see on Figure 8 a) and b). when the weld toe radii is increased, Figure 8 c), d) and e), the hammer peening tool tip can now be directly place on the weld toe, so the residual stress distribution is very similar.

When one looks at the residual stress values on the weld toe in every direction, Table 7, it is possible to confirm the above referred behavior, with the highest differential occurring in the direction of the thickness.

**Table 7 Residual Stress vs. Specimen weld toe radii**

Specimen (Weld Toe)	$\sigma_{XX}$ [MPa]	$\sigma_{YY}$ [MPa]	$\sigma_{ZZ}$ [MPa]
ProvAvg02Std	-594.9	-202.9	-595.0
ProvAvg01Std	-433.7	-123.2	-399.2
ProvAvg	-538.9	-116.8	-506.9
ProvAvg1Std	-558.4	-136.4	-563.1
ProvAvg2Std	-537.1	-142.4	-550.0

**Table 8 Experimental and numerical Residual Stress on the weld toe [MPa]**

	Weld Toe Long.	Weld Toe Transv.	1 mm Long.	1 mm Transv.
Experimental	-485 ± 31	-524 ± 26	-269 ± 9	-162 ± 18
Numeric	-539 ± 60	-507 ± 76	-300 ± 73	-93 ± 22
Diferential	11%	-3%	12%	-43%

When compared with the residual stresses obtained experimentally by the X-Ray diffraction technique, Table 8, one can see that the values show a good agreement. On the weld toe, the residual stresses obtained experimentally and the numerical value obtained with the specimen created using the average weld toe radii only differ 11% in the longitudinal direction and 3% on the transverse direction. When the values are obtained 1 mm away from the weld toe, the relative difference in the transverse direction is higher, but it must be taken into account that the residual stresses in this direction have a lower absolute value. Therefore it is possible to validate the numerical model.

### 3.2 Fatigue Data in the Welded Joints

Having analyzed the residual stresses after the hammer peening technique, one can apply several fatigue cycles to the specimen, in order to simulate the fatigue life tests applied to real specimens. These cycles have constant frequencies, and stress ranges, with a stress ratio of 0.1.

Table 9 therefore shows that the local stress and strain range is not significantly influenced by the weld to radii. The biggest difference is 6.8% between the strain range obtained with the average weld toe radii and the minimum one. When the mean stress is analyzed the differentials are higher, and the influence of the weld toe radii more clear. For the minimum radii, the mean stress is 32.5% lower in modulus than the solution obtained with the average radii, so one can expect a shorter fatigue life. When the radii is increased the mean stress decreases about 11.9%, which can lead to a higher fatigue life. The nominal loading also has the expected behavior, changing not only the stress and strain range values, but more significantly the mean stress value.

**Table 9 Weld toe local stress range, mean stress and strain range vs Specimen weld toe radii**

Specimen	$\Delta\sigma_{XX}$ [MPa]	$\sigma_{mXX}$ [MPa]	$\Delta\epsilon_{XX}$ [ $\mu$ ]
ProvAvg02Std	377.8	-125.2	2103
ProvAvg01Std	374.7	-145.4	2060
113 MPa	177.9	-303.0	958
ProvAvg 225 MPa	365.1	-185.7	1969
400 MPa	510.9	-81.4	2756
ProvAvg1Std	375.6	-155.1	2016
ProvAvg2Std	357.5	-207.7	1920

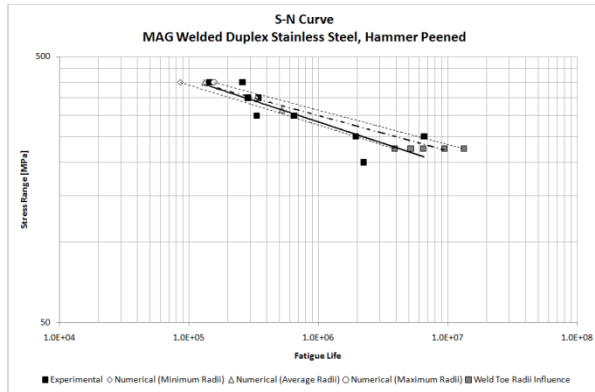


**Figure 9 S-N curves experimentally and numerically obtained for the Duplex Steel**

Using the above results and the local approach method it was then possible to calculate the fatigue life initiation, as *Pinho-da-Cruz et al* in [19], *Silva et al* in [20], have testified, and therefore create the S-N curves from Figure 9. Three numerical S-N curves were calculated, using the minimum, average, and the maximum weld toe radii values. It is very interesting to see that the experimentally obtained S-N curve fits between the minimum and maximum radii S-N curves, which mean that the numerical model is working well, and is able to correctly predict the fatigue life initiation.

Comparing only the experimental S-N curve with the average radii one, one can see the numerical solution is not conservative, and therefore always predicts a higher fatigue life. But when one uses the minimum radii values, the S-N curve will now predict a lower fatigue life, and therefore the numerical results are now conservative.

Table 10 shows the numerical results obtained using the FEA model, need for the fatigue life initiation prediction. The influence of the weld toe radii can also be quantified, like in [21] by *Chin-Hyung Lee et al*, using a 225 MPa stress range fatigue cycle, and several different radii. With the minimum weld toe radii the predicted fatigue life is 3'888'753 cycles, increasing to 9'445'579 cycles, when the radii changes from 1.053 mm to 2.420 mm. Increasing the radii 56.5% again, the fatigue life increases to 13'302'658 cycles, which represents a 41% change. On average the weld toe radii changes the fatigue life prediction by 30%.

**Table 10 Fatigue Life Prediction for the Duplex Steel after weld toe hammer peening,  $\Delta S=225$  MPa**

Specimen	$\sigma_m$ [MPa]	$\Delta\epsilon$ [ $\mu$ ]	Ni [Cycles]
ProvAvg02Std	-125.2	2100	3888753
ProvAvg01Std	-145.4	2060	5175726
ProvAvg	-185.7	1970	9445579
ProvAvg1Std	-155.1	2020	6452840
ProvAvg2Std	-207.7	1920	13302658

### 4 Conclusions

- In order to model the hammer peening technique it was necessary to determine the hammering force, this value was then applied to the FEA model. an instrumented hammer peening tool was used and a – 720 N average force, or an equivalent – 7 MPa hammering pressure was determined;
- The hammer peening technique is based not only on the modification of the weld toe radii, but also in the introduction of a residual compression stress distribution on the weld toe;
- Several factors were analyzed in the FEA model, like the number of strokes per specimen, the orientation of the hammer peening tool, the hammer peening tool geometry or the hammer peening applied force;
- As expected the residual stress distribution through the specimens thickness has two inflection points, the first one, near the material surface, where the higher residual stress value is obtained, and the second one, at a depth of 1 mm to 2 mm, where the residual stresses are now on the positive side;
- By adding the residual stress distributions to the nominal load stress profiles, it is possible to conclude that the resulting stress range decreases, while the strain range is slightly increased, the mean stress value

is also considerably decreased when compared with the as welded condition;

- Based on these values it is possible to predict the fatigue life, for the as welded and hammer peened conditions, attesting therefore the efficiency of the hammer peening technique as an fatigue life improvement technique;
- There is a very good agreement between the experimental and the numerically obtained S-N curves, while altering the hammer peening tool radii proves to be an effective way improve this agreement;

### ACKNOWLEDGEMENTS

The authors acknowledge: TWI for the financing of the "Improving the fatigue performance of welded steels", ECSC Contract 7210 – PR – 303.F3 project; The FCT for the PhD scholarship SFRH/BD/25984/2005 financing support.

### REFERENCES

- [1] Infante, V., Branco, C.M., "A comparative Study of the Fatigue Behaviour of Repaired Joints by Hammer Peening", Paper XIII-1836-2000
- [2] Dexter, R.J., Kelly, B.A., "Research on Repair and Improvement Methods", Proc. 50<sup>th</sup> Annual Assembly, San Francisco, EUA, WRC, 1997, pp. 74-97
- [3] Baptista, R.M., "Estudo dos parâmetros de martelagem no comportamento à fadiga de juntas soldadas de aço estrutural", Tese de Mestrado em Engenharia Mecânica, IST, Julho 2002
- [4] Infante, V., "Análise da melhoria do comportamento à fadiga de juntas soldadas", Tese de Doutoramento em Engenharia Mecânica, IST, Abril 2002
- [5] Infante, V., Branco, C.M., Baptista, R., Gomes, E.C., "Residual stresses and fracture mechanics analysis of welded joints repaired by hammer peening", Proc. 8<sup>th</sup> Portuguese Conference on Fracture, Vila Real, UTAD, Ed. SPM, Lisboa, pp. 339-354, Março 2002
- [6] Infante, V., Branco, C.M., Baptista, R. "Failure analysis of welded joints rehabilitated by hammer peening", Paper XIII 1892/01, IIW Meeting, July 2001, Ljubljana, Slovenia, Ed. International Institute of Welding
- [7] TWI, "Improvement the Fatigue Performance of Welded Stainless Steels", Final Report for contract No. 7210-PR-303, 2005
- [8] Huther, I., Lieurade, H.P., Sonissi, R., Nussbaumer, A., Chabrolin, B., Janosh, J.J., "Analysis of Results on Improved Welded Joints", Welding in the World, 37, 5, pp. 242-266, 1996.
- [9] Maddox, S.J., "The Application of Fatigue Life Improvement Techniques to Steel Welds", IIW Commission XIII Workshop on Improvement Methods, International Institute of Welding, Proc. 51<sup>st</sup> Annual Assembly, Hamburg, Germany, September 1998.
- [10] Haagensen, P.J., Maddox, S.J., "Specifications for Weld Toe Improvement by Burr Grinding, TIG Dressing and Hammer Peening for Transverse Welds", IIW Document, Commission XIII, Working Group 2, WG2, International Institute of Welding, 2001.
- [11] B. Atzori, G. Meneghetti, "Fatigue strength of fillet welded structural steels: finite elements, strain gauges and reality", International Journal of Fatigue 23 (2001) 713-721
- [12] Wolfgang Fricke, "Fatigue analysis of welded joints: state of development", Marine Structures 16 (2003) 185-200
- [13] Lemaitre, J., and J.-L. Chaboche, *Mechanics of Solid Materials*, Cambridge University Press, 1990.
- [14] Jean-Christophe Le Roux, "Étude Du Comportement Et De L'endommagement En Fatigue D'un Acier Inoxydable Austéno-Ferritique Moulé Vieilli", These.
- [15] Dowling, N.E., "Fatigue at Notches and Local Strain and Fracture Mechanics Approaches", ASTM, STP 677, pp. 247-273, 1979
- [16] J. D. Morrow, "Cyclic Plastic Strain Energy and Fatigue of Metals, Internal Friction, Damping and Cyclic Plasticity", *ASTM-STP* 378, 45-87 (1965)
- [17] Rodrigo Magnabosco, Gustavo Henrique Bolognesi Donato, "Comportamento Mecânico Monotônico E Cíclico De Dois Aços Inoxidáveis Dúplex", 59<sup>o</sup> Congresso Internacional Anual da ABM – São Paulo, 19 a 22 de Julho de 2004
- [18] J. Liu, W.X. Gou, W. Liu, Z.F. Yue, "Effect of hammer peening on fatigue life of aluminum alloy 2A12-T4", *Materials and Design* xxx (2008) xxx-xxx
- [19] J. Pinho-Da-Cruz, F. Teixeira-Dias, P. S. Ferreira, "Aplicação Dos Métodos De Aproximação Local E Elementos Finitos À Previsão De Tensões-Deformações Em Provetes Entalhados De Alcu4,5mn", *Revista Iberoamericana De Ingeniería Mecánica*. Vol. 10, N.º 1, pp. 93-110, 2006
- [20] V.R. Silva, J.D. Costa, J.M. Ferreira, "Fatigue Crack Initiation in Central Notch Specimens of 6082-T6 Aluminium Alloy", 8<sup>a</sup> Jornadas da Fractura – 2002, pp. 255-263
- [21] Chin-Hyung Lee, Kyong-Ho Chang, Gab-Chul Jang, Chan-Young Lee, "Effect of weld geometry on the fatigue life of non-load-carrying fillet welded cruciform joints", *Engineering Failure Analysis* 16 (2009) 849-855